Supporting Information

Solvent-free Strategy Yields Size and Shape-uniform Capsules

*Ana M. S. Costa and João F. Mano**
Department of Chemistry, CICECO, Campus Universitário de Santiago, University of Aveiro, 3810-193 Aveiro, Portugal
*E-mail: jmano@ua.pt

MATERIALS:

Glass microscope slides were from Medline (Spain). Poly(L-lactic acid) (PLLA; Mw ~1600−2400, 70% of crystallinity) was purchased from Polysciences (Germany). Methylene chloride (CH_2Cl_2) was obtained from Fisher Chemical (U.K.). Polyvinyl alcohol (PVA), tetraethyl orthosilicate (TEOS, 98%), ammonium hydroxide solution (30-33%), 1H,1H,2H,2H-perfluorodecyltriethoxysilane (silane, 97%), ethylenediaminetetraacetic acid (EDTA), 2-hydroxy-4'-(2- hydroxyethoxy)-2-methylpropiophenone (I2959, 98%), methacrylic anhydride (MA, ≥92%), phosphate buffer saline (PBS), penicillin/streptomycin solution, ethanol (EtOH), sodium carbonate (Na_2CO_3, ≥99.5%), calcium chloride ($CaCl_2$, ≥96%), low viscosity sodium alginate from brown algae (ALG, ~250 cP), antibiotic/antimycotic, gelatin from porcine skin, glycerol (≥ 99%), iron(II) chloride tetrahydrate (ferrous, $FeCl_2.4H_2O$, 98%), iron(III) chloride hexahydrate (ferric, $FeCl_3.6H_2O$, 98%) and 2-(N-morpholino)ethanesulfonic acid hydrate (MES, ≥99.5%) were from Sigma-Aldrich (U.S.A.). Chitosan 95/20 was from Heppe Medical Chitosan GmbH (Germany). Acetic acid (Glacial) was supplied from VWR (Belgium). TrypLE Express were from Alfagene (Portugal). Fibroblast Growth Kit (L-glutamine, hydrocortisone hemisuccinate, rh FGF β, rh EGF/ TGF β1 supplement, rh insulin, ascorbic acid and HLL supplement, which in turn contained human serum albumin, linoleic acid and lecithin) was obtained from ATCC (U.K.). Fetal bovine serum was obtained from Merck Milipore (U.S.A). LIVE/DEAD Viability/Cytotoxicity Kit was from Molecular Probes Invitrogen (U.S.A.). Dyes (E102, E129, E133) were purchased from Elveflow (France). All materials were used as received. Unless otherwise stated, water purified in an 18 MΩ cm MilliQ Plus water system was used throughout.

METHODS:

S1. Preparation and Characterization of Polymeric Capsules using Alginate as a sacrificial template

Most of the technologies employed to fabricate hydrogel spheres are produced in a liquid environment (under “wet-conditions”) for example, by precipitation/crosslinking in a coagulation bath or by emulsion, in which a liquid polymeric precursor hardens into its hydrogel form upon immersion in another insoluble liquid substrate. Herein, hydrogel capsules were produced basically in a liquid-air interface by using superamphiphobic surfaces, as shown schematically in Figure S1. When suspended over these substrates, a liquid droplet acquires a spherical shape, which can be then retained by applying a crosslinking step without being in contact with any other liquid media. Therefore, this strategy is solvent-free since there is no need for any external liquid environment because in all the steps the drop is basically involved by the atmospheric environment and the contact with the solid substrate cover a negligible area. Moreover, most of the current available synthesis routes require the use of organic liquids and involve different steps to obtain the final particles, hampering the encapsulating of sensitive cargoes, such as living cells. In this work, we propose a new method that enables us to encapsulate highly sensitive and unstable compounds in spherical hydrogels particles with high efficiency and under mild conditions, enabling the creation of novel platforms that could have direct applicability in different areas such as the biotechnological and biomedical fields.

S1.1. Fabrication Process of Polymeric Capsules

Liquid-core methacrylamide chitosan (MACHI) capsules were fabricated as shown on Figure 1 (see article). First, controlled volumes of a 1.5% (w/v) alginate (ALG) in water solution (pH 7.0) were dispensed over a superamphiphobic (SA) substrate using a pipette. Different volumes were tested in order to tune the particle size. The obtained

pre-gel droplets were subsequently hardened into a hydrogel upon adding other droplet containing Ca^{2+} ions (ionotropic gelation, 0.1 M $CaCl_2$ in 25 mM MES solution, pH 7.0) for 15 min in a humidified atmosphere to prevent water evaporation. It is worth noticing that, only for visualization purposes, the obtained ALG microparticles were stained by introducing a food dye in the polymer precursor solution (E133, 0.1% (v/v) in water, stains in dark blue). In order to produce polymeric capsules using ALG as sacrificial template, a droplet of MACHI polymer (2% (w/v) in a 16% (v/v) glycerol/water solution containing 0.25% (w/v) I2959, pH 7.0) was dispensed above a SA surface. With the aid of superhydrophobic tweezers, the ALG hydrogel core was entrapped within the previous droplet followed by its exposure to UV-light (365 nm, 2.8 mW/cm^2) for 1 min. Finally, the cross-linked ALG core was dissolved by performing a EDTA treatment (0.02 M in a 25 mM MES buffer solution, pH 7.0) for 5 min, yielding liquefied MACHI capsules. The obtained ALG cores and MACHI capsules were observed using an optical stereomicroscope (Stemi 508, Zeiss, Germany) equipped with a digital camera and characterized for their morphology, size and size distribution by measuring the diameter of 12 particles obtained in three different experiments using ImageJ^{TM} software.

S1.2. Alginate polymer and Reversible Crosslinking Process

ALG, a polysaccharide mainly obtained from brown algae, is a linear copolymer composed of consecutive blocks of (1-4)-linked β-D-mannuronic acid (M-blocks) or its C-5 epimer α-L-guluronic acid (G-blocks) monomers or alternating M and G-residues (M-G blocks). This natural polymer tends to be negatively charged at a pH of around 7.4 (the physiological pH) since its pka value is of 3.4 and 3.7 for M and G acids, respectively. [1] Thus, ALG can yield gels when the carboxylic acid groups present on its backbone come into contact with divalent cations such as calcium ions. This bond occurs between G-blocks of adjacent ALG chains during gelling, creating an egg-box-like structure.[2, 3] In order to ensure the effective interaction between ALG and Ca^{2+} ions, several parameters such as the polymer and ion concentrations, and pH value need to be optimized. The

values chosen were already reported in other publications.[4] A unique characteristic of ALG is its ability to reverse its gelling process, meaning that it is possible to return to ALG non-crosslinked form (liquid state), by simply adding Ca^{2+} chelators such as ethylenediamine tetraacetic acid (EDTA).[5, 6] The selected amount and time of EDTA treatment was based on other publications and was proved to be efficient in liquefying the ALG core.[4] All of these characteristics make ALG a great candidate to fabricate the capsule' liquid core under mild conditions.

S1.3. Preparation and Characterization of Superamphiphobic Surfaces

The methodology followed to produce these SA surfaces has already been reported in literature.[7-9] In short, glass slides were soot coated above a paraffin candle followed by a CVD procedure within a desiccator containing both TEOS solution (4 mL) and ammonia (4 mL). Calcination of the coated substrates was performed 24h after the CVD procedure by placing them at 550ºC for 2h. Immediately after, the obtained surfaces were exposed to another CVD process using a silane solution (150 µL) for 3 days and stored until use. These substrates were previously characterized by others and us[7-9] in terms of their morphology, topography and water contact angle (WCA) by Scanning Electron Microscopy (SEM), Atomic Force Microscopy (AFM) and static WCA measurements, respectively. Herein, we extended the topographic characterization by using a profilometer. To this end, the samples were covered with a carbon layer to render them opaque to light and after analyzed to assess its roughness (root mean square - RMS value) using the SensoSCAN 5.3 software supplied with this equipment. The surface microstructure was also determined from the aforementioned images by drawing intensity plot profiles across the obtained pictures and defining a threshold. The distance between two peaks was defined as the micro-feature size. Results are the mean of 20 measurements using 10 different intensity plots.

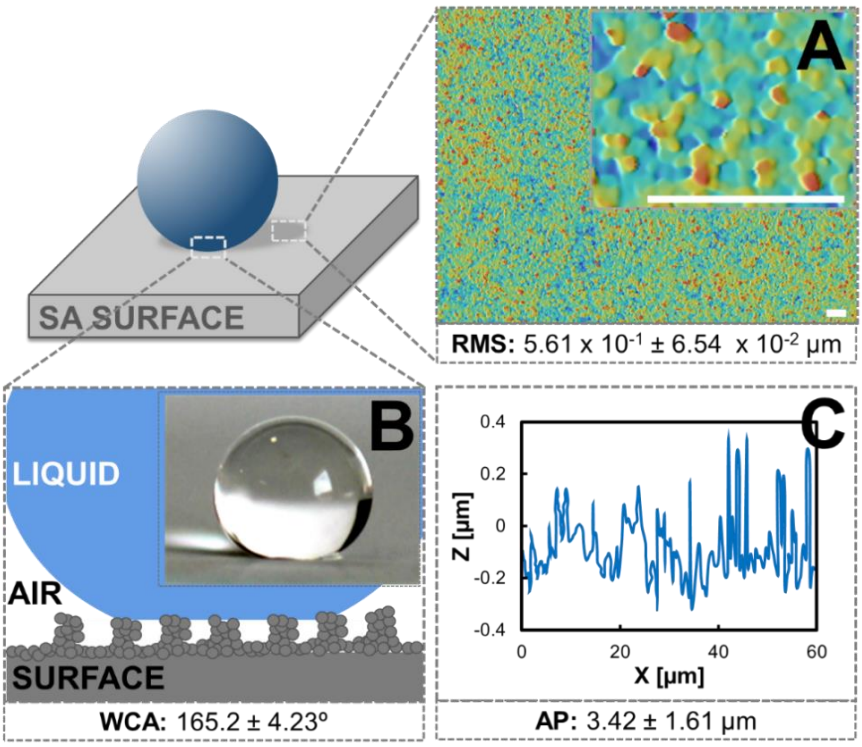

Figure S1. Wettability character of the produced SA surfaces. **(A)** Representative topographic image obtained using a profilometer, depicting the surface roughness (RMS) value. The scale bar corresponds to 1 µm. The inset contains a zoom in of a certain region of the former image. The scale bar corresponds to 0.5 µm. **(B)** Schematic representation of a liquid droplet deposited on the fractal-like composite interface of the produced SA substrates. Inset corresponds to a lateral view of a 3 µL water droplet deposited on the SA surface. **(C)** Z profile of SA surfaces obtained all along the X-axis at a fixed Y-coordinate, showing the average pitch (AP) size values, as determined from these surfaces.

Moreover, the static WCA was assessed in order to confirm the wettability of the produced substrates and was conducted on the basis of the sessile drop method. In a typical experiment, 3 µL water droplets were dispensed over a SA surface and the angles were measured after drop stabilization using the SCA 20 software. The experiments correspond to three replicates carried out on ten different surface regions at room temperature (RT). The shape factor (SF) of the produced droplets was determined from

their lateral view and used to further confirm their sphericity. Indeed, SF was calculated as the ratio between the orthogonal and parallel diameters in relation to the SA surface. A superhydrophobic (SH) substrate is defined by a WCA value greater than 150º,[10] which is conferred by the presence of both surface roughness (usually originated from microscopic protrusions with nano-scale features) and a low surface energy.[11] A behavior like this can be found in Nature, where several structures are able to repel water such as the case of the lotus leaf and its associated self-cleaning character, and also the case of the water strider's leg.[12, 13] Regarding the hierarchical structure, it is well known that the presence of microstructures allow the resistance to the capillary waves whilst the nanostructures are able to prevent the valleys filling by small droplets.[14] Besides these features, if a surface also exhibits overhanging structures, it can also repel oleo-based liquids, yielding SA surfaces.

The surface topography was analyzed using a profilometer in order to get an insight into the height of the microprotusions as well as the spacing between the asperities, which as already mentioned are critical to attain a SA character. Figure S1 displays the obtained results, suggesting the presence of a rough architecture resulting from the deposition of carbon particles (soot layer) with RMS values of 0.561 ± 0.065 mm. This outcome proves the successful modification of the microscope slides leading to the formation of microstructures, which were found to be homogeneously distributed over the entire SA substrate. Owing to this surface topography, when a water droplet is placed in contact with a SA surface, it exhibits a spherical shape. This shape is the result of the entrapment of air in the valleys between the microscopic protrusions above which the droplet is suspended in the Cassie state and, consequently, avoid its collapse into the Wenzel wetting state. Therefore, this composite interface (solid-air-liquid) leads to an increase in the macroscopic contact angle and a reduced contact angle hysteresis. Indeed, the WCA angle was measured to assess the extent of droplet contact with the SA surface and the obtained results are displayed in panel S1B. The high WCA values obtained, around 165º, reflect the low contact area of the droplet with the produced SH

substrates, in compliance with other results found in literature.[8, 9] Figure S1B inset shows an example of a droplet observed from the side view. By observing this image is possible to notice the characteristic spherical shape, which was further proved by the SF value obtained, which close to 1. Together with RMS, this network-like structure is responsible for promoting a higher WCA as well as a more stable composite solid-liquid-air interface. In order for the surface features to readily promote the formation of this interface, they must present nominal pitches smaller than the actual diameter of the given droplet. As observed on Figure S2C, textural features resulting from this surface coating present average pitches of around 3.42 ± 1.61 mm, proving themselves as suitable resting places for the produced micro-droplets.

In sum, the characterization of these superamphiphobic surfaces was further extended by using a profilometer to assess the surface roughness. Although this technique has a lower resolution when compared with others such as Atomic Force Microscopy (AFM), it is quite simple as it does not require the adjusting and/or optimization of multiple parameters as well as rapid since it takes short acquisition times. Interestingly, the obtained roughness (RMS; root mean square) values were not significantly different from the ones reported on literature ($p<0.5$; 0.498 ± 0.072 vs 0.56 ± 0.065 mm for AFM and profilometer, respectively). In sum, the characterization of the WCA and the magnitudes obtained thereof further confirm the right formation of the SA substrates.

Importantly, due to the simultaneously superhydrophobic and superoleophobic character of the used substrates, the capsules may contain virtually any type of liquid make it possible to broad the application spectrum to diverse technological purposes such as agriculture, biotechnology, cosmetics, and electronics, where solvents different than water are often required.

S1.4. Capsule Size and Density Mismatch: Glycerol and Hydrophobic Tweezers

The size of the produced hydrogel spheres can be controlled by dispensing precise volumes of the liquid using a micropipette. As shown on Figure 1a, the volume varied

from 2 µL (minimum volume of ALG solution that was possible to dispense using a micropipette due to viscosity and surface tension constraints) to 8 µL (maximum volume of ALG solution dispensed to, after the addition of the MACHI polymer, avoid gravity effects on the capsule shape), corresponding to core diameters ranging between *ca.* 0.4 mm and 1 mm. Smaller particles may be obtained using spray-based methods or using other dispensing systems, which furthers strengths the importance of the dispensing mechanism used to tune the droplet size.[8,9] The lower size limit is determined by various factors such as the dispensing method employed (*e.g.* spraying,...), the solution properties (*e.g.* viscosity,...), the substrate features (*e.g.* the distance between asperities on the surface) and the external conditions applied (*e.g.* pressure,...).[11] It was shown that for relatively small volumes the shape of liquid drops on an extremely water repellent surface is almost spherical, tending to a more deformed geometry for the case of bigger droplets due to the effect of gravity, which is the main limiting factor to obtain bigger spherical particles. Herein, the capsule size ranged from *ca.* 500 µm to 2 mm since, besides the core size, the capsule also has a shell thickness. Moreover, after the conversion of the polymeric droplet into a crosslinked particle, the size can also be different from the one of the initial droplet, due to the typical occurrence of shrinking during the crosslinking process and/or due to water evaporation from the droplet, for example. To avoid these former problems, the particle size was measured after 15 min of Ca^{2+}-mediated crosslinking and by incubating the particles under a humidified atmosphere. Regarding the shell thickness, it is challenging to attain a value lower than 100 µm due to the dispensing method used (by pipetting) and to ensure that the core was exactly in the middle position (Figure S2).

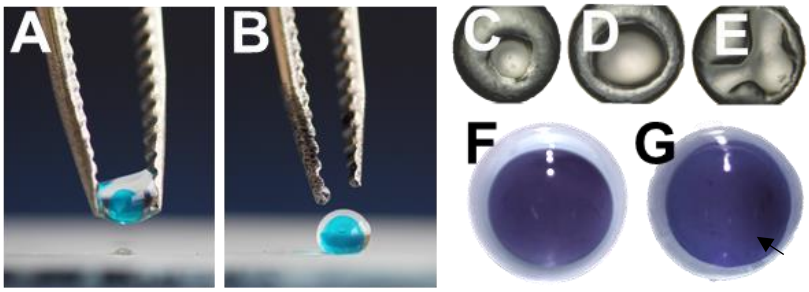

Figure S2. Placement of a ALG crosslinked core (E133, stained in blue) inside a MACHI droplet using non-modified **(A)** and hydrophobic tweezers **(B)**. Due to the high repellency of the produced SA surfaces, the tweezers were modified using a waterproof spray to enable the deposition of the core within the MACHI droplet, as otherwise, the droplet would remain attached to them. **(C)** This step should be carried out in the presence of glycerol to avoid the sank of the ALG core into the surface, which may result on the formation of a hole after UV-mediated crosslinking. Moreover, owing to the low dimensions of this molecule, it is expected that once in solution glycerol will be able to diffuse into the surrounding medium, being released from the produced polymeric structures. **(D)** Typical appearance of the middle section of a MACHI particle by using glycerol. It is possible to observe that the produced capsule is hollow, resulting in a compartment that can be loaded with different compounds. **(E)** Other issue that need to be controlled is the stability of the capsule, which can be accomplished by increasing the UV-mediated crosslinking. After 20 s of UV crosslinking, a capsule is formed but it is not sufficiently robust to maintain its spherical shape, resulting on its collapse. **(F)** The sacrificial core must occupy the middle position in both directions vertical and horizontal in order to ensure a homogenous thickness, being critical for lower shell thickness (**G**, arrow).

S1.5. Methacrylamide Chitosan synthesis process, characterization and UV-mediated crosslinking

CHI, a polycationic biopolymer widely used in the biomedical field, is attractive because of its biocompatibility and chemical versatility.[15] Herein, 3 %(w/v) CHI was dissolved in 2 %(v/v) acetic acid overnight at RT with constant stirring as previously reported on literature. [16] Afterwards, MA was added at 0.4 molar equivalents per chitosan repeat unit

and left for 3h at RT. The mixture was dialyzed against distilled water for 7 days, changing the water twice a day. The MACHI solution was, then, freeze-dried and stored at -20ºC until use. Fourier Transform InfraRed Spectroscopy (FTIR, Bruker Tensor-27) was used to infer about the correct CHI methacrylation. Transmission spectra for both CHI and MACHI were recorded using the ATR mode (Golden Gate Acccessory, SPECAC) within the range of 4000-400 cm^{-1} using 256 scans, with a resolution of 4 cm^{-1}. Figure S3 reveals that the IR spectra of CHI shows the typical peaks of each component, namely the CH bands at ca. 3700-2900 (-NH_2 and -OH groups); 2872 (-CH_2-); 1648 and 1581 (amide I and II, respectively); and 1058 (C-O) cm^{-1}.[17] Meanwhile, the MACHI spectrum displays, in addition to those characteristic of CHI, the appearance of one distinctive peaks of MA (marked with arrows) at 1606 cm^{-1}. As previously demonstrated for the methacrylation of dextran, this band correspond pendant vinyl groups (the next two). [18, 19] Taken together, these findings demonstrate that the CHI modification was successfully executed.

Moreover, the influence of the UV-crosslinking time on the crosslinking degree was also assessed. As a result of the UV-light exposure, the photoinitiator forms free radicals needed to initiate the polymerization process, namely the reaction between the methacrylated pendant groups on the MACHI. Therefore, the crosslinking degree of the MACHI was evaluated by the disappearance of the vinyl methylene groups on IR spectrum, after normalizing all the spectra. It is important to notice that FTIR was only used to evaluate qualitatively this process driven by UV-light. Its quantification was already provided in a previous publication resorting to NMR.[8] After 1 min, the characteristic peak of the methacrylic groups was still present but was lower, suggesting that MACHI chains have been crosslinked in order to create a hydrogel network. By contrast, after 15 min this peak was almost completely removed, suggesting that almost all the groups were consumed to create a 3D-network. This results are in good agreement with previous publications. [9]

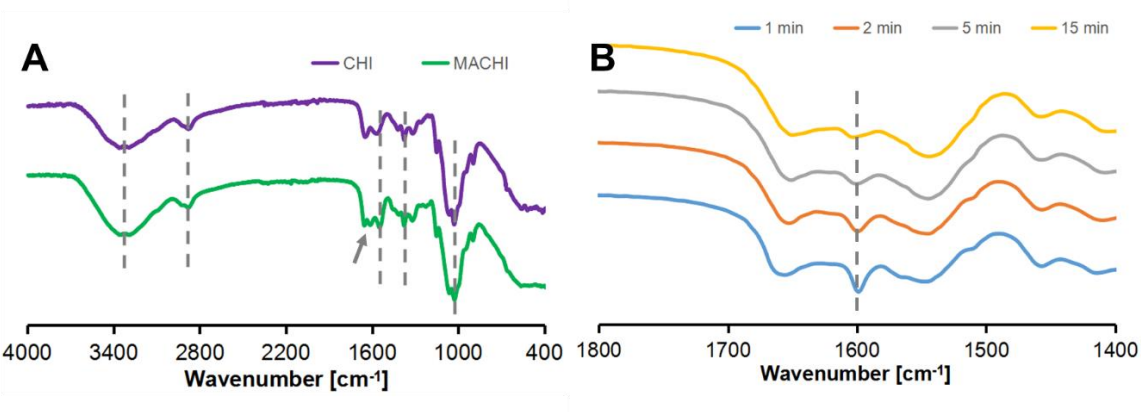

Figure S3. (A) FTIR spectra of chitosan (CHI) and methacrylamide chitosan (MACHI). Marked with an arrow is the methacrylic group from MACHI polymer, which was attached to the modified CHI polymer. **(B)** FTIR spectra of MACHI polymer after its exposure to UV-light for 1,2,5 and 15 min. The decreasing of the characteristic (C=C) characteristic peak over time suggests the formation of a crosslinked 3D-structure. Results are presented in %T.

S2. Cell encapsulation inside Polymeric Capsules

S2.1. In Vitro Cell culture

Human adult primary dermal fibroblasts (ATCC® PCS-201-012™) were cultured in a Fibroblast Growth Kit medium supplemented with 10% FBS (heat-inactivated) and 1% penicillin-streptomycin (pH 7.4). Cells were grown in 150 cm^2 tissue culture flasks and incubated at 37 ºC in a humidified air atmosphere of 5% CO_2. The culture medium was exchanged every 3 days.

S2.2. Fibroblast encapsulation within MACHI capsules

Upon reaching 90% of confluence, fibroblasts were washed with PBS and chemically detached from tissue culture flasks using 0.05% Tryple Express solution for 5 min at 37ºC in a humidified air atmosphere of 5% CO_2. Later, fresh medium was added to inactivate the Tryple Express effect and the cells were centrifuged at 1200 rpm for 5 min.

Then, the medium was decanted followed by the cells re-suspension in different polymer in MES solution (pH 7.4) at a density of $1x10^6$ cells per mL of polymer solution.

Five different formulations were tested as depicted on Figure S3: the first condition (A: ALG core+Cells) was done to study the ability of the produced ALG cores to entrap cells with high viability rates and was performed by ressuspended cells in 1.5% (w/v) ALG solution followed by Ca^{2+}-mediated crosslinking for 15 min (ionotropic gelation, 2 µL of 0.1 M $CaCl_2$) in a container with saturated humidity; the second condition (B: (ALG core+Cells) + MACHI shell) was performed in order to evaluate the effect of a MACHI external matrix on viability of cells entrapped within ALG crosslinked particle and was performed by entrapping a (ALG core+Cells) within a 2% (w/v) MACHI droplet containing 0.25% (w/v) I2959 photoinitiator and 16% (v/v) glycerol followed by UV curing for 1 min; the third condition (C: ((ALG core+Cells) + MACHI shell) + EDTA) was done to assess the effect of dissolution of the ALG core inside the MACHI shell on cell viability and was performed by adding a droplet of EDTA solution (chelating agent, 6 µL of 0.02 M) above a ((ALG core+Cells) + MACHI shell) for 5 min; the forth condition (D: MACHI particle + Cells) refers to the control of the ability of cells to maintain viable after their encapsulation within a MACHI matrix and was performed by ressuspend the cells within a 2% (w/v) MACHI droplet containing 0.25% (w/v) I2959 photoinitiator and 16% (v/v) glycerol followed by UV curing for 1 min. Finally, the fifth condition (ALG core + (MACHI shell+Cells) + EDTA) constitute the control of the presence of ALG liquefied core on the cell viability within the MACHI shell and was performed by incorporating an ALG core within a MACHI droplet containing cells followed by UV curing for 1 min. The sacrificial core was obtained from a 2 µL droplet of a ALG pre-gel solution whereas a 4 µL droplet of a MACHI precursor solution was used to produce the polymeric shell. The MACHI + Cells particles (E) were done by dispensing a 6 µL droplet above a SA surface in order to attain the same size as the one of the polymeric capsules. Then, the produced particles were placed inside a 12-well tissue culture plate at 37ºC with a humidified air atmosphere of 5% CO_2.

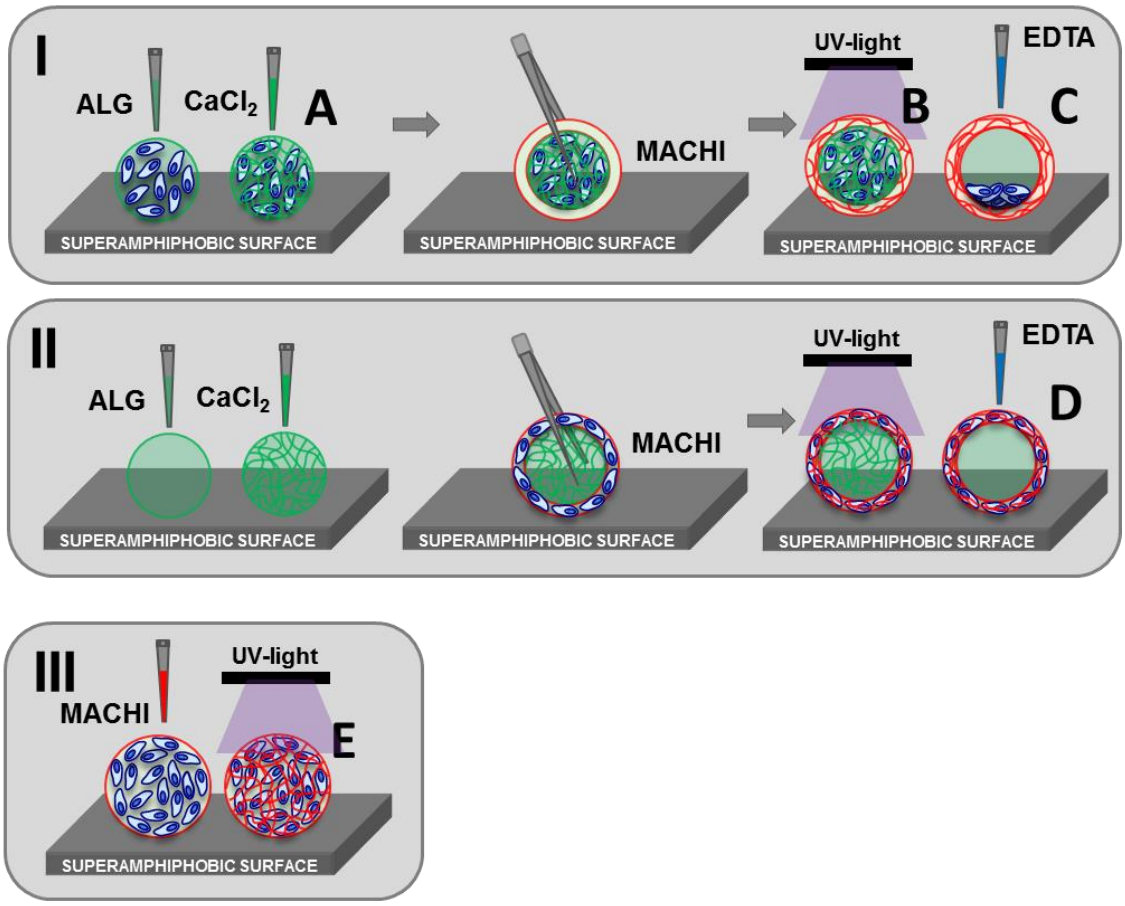

Figure S4. Schematic representation of the synthesis route to attain cell-laden carriers. **I)** Cell-laden ALG cores were crosslinked upon adding Ca^{2+} ions **(A)** and assembled into a MACHI droplet over a SA surface using superhydrophobic tweezers. Afterwards, the MACHI matrix was crosslinked by UV-light exposure **(B)** followed by the ALG core removal after a EDTA treatment, yielding MACHI capsules with a liquid-core containing cells **(C)**. **(II)** Non-loaded ALG core was also incorporated into a droplet of MACHI with cells as stated before in order to obtain cell-laden MACHI capsules with a liquid-core **(D)**. **(III)** Cell-laden MACHI carriers were also produced by suspending cells in this polymer precursor solution followed by its dispensing over a SA surface using a pipette and, its subsequent crosslinking by UV-light exposure **(E).**

S2.3. Cell Viability Assessment: LIVE/DEAD Assay

After 24h, the effect of the developed technology on the cell viability inside the different five formulations was qualitatively assessed by performing a LIVE/DEAD assay. This assay is based on the ability of viable cells' esterases to hydrolyze calcein-AM

(membrane permeant dye) into calcein (green fluorescent dye), which is retained inside the cytoplasm. In turn, ethidium homodimer (EthD-1, red fluorescent dye) binds mainly to DNA of disrupted cells since it is membrane impermeant. Briefly, the culture medium was removed and replaced by 1 mL of PBS containing 0.5 µL of a 4 mM calcein AM stock solution and 2 µL of a 2 mM EthD-1 stock solution. After 30 min of incubation at RT, samples were washed three times with PBS and visualized immediately after by a fluorescence microscope (Z1m Inverted Microscope, Zeiss, Germany) using excitation and emission wavelengths of 494 and 535 nm and 517 and 617 nm for calcein-AM and EthD-1, respectively. These experiments were repeated three times for each sample.

S3. MACHI particles: Multiple template cores

Although the attained polymeric shell directly determines the capsules properties and, hence, their application, the template choice also plays an important role on the final characteristics of the obtained capsules as their size and shape are mainly dictated by the used sacrificial core.[20, 21] Therefore, special attention should be paid to the core composition, processing conditions and stability to allow its assembly within the MACHI droplet as well as to provide the appropriate conditions for its removal to not jeopardize the structure of both the capsule shell and the cargo.[22-24] In light of these facts, different templates along with different core removal methods were tested to evaluate the versatility of the developed strategy to obtain polymeric capsules with different physicochemical characteristics and, hence, making it possible their application in distinct fields. A schematic representation of the various strategies developed is shown on Figure 3 (see article).

S3.1. Thermosensitive-Cores

S3.1.1. *Gelatin*

Gelatin is well-known for its biocompatibility, biodegradability and non-immunogenicity as well as for exhibiting cell-adhesive motifs all along its backbone. [25-27]

A 2 µL droplet of a 2% (w/v) gelatin in water solution (with food dye 50:50 E133/E129, 0.1% (v/v) in water, stains in purple) was dispensed over a SA surface and, subsequently, harden into a hydrogel by decreasing the temperature to 4ºC. Afterwards, a 2% (w/v) MACHI in water solution containing 0.25% (w/v) of I2959 photoinitiator and 16% (v/v) glycerol solution (with food dye E129, 0.01% in water, stains in light red) was used to produce a polymeric shell around the gelatin sacrificial core upon its UV-light crosslinking (365 nm, 2.8 mW/cm^2) for 1 min. The gelatin crosslinked core was turned into a liquid by increasing the temperature to 37ºC, yielding in liquid-core MACHI capsules.

S3.1.2. *Ice*

A 2 µL water droplet containing a food dye (E129, 0.1% (v/v) in water, stains in red) was deposited above a SA surface and, subsequently, frozen at -80ºC for 15 min. Meanwhile, MACHI polymer was dissolved in 15% (v/v) EtOH in water solution (2% (w/v)) containing 0.25% (w/v) I2959 photoinitiator and placed at 4ºC. Polymeric capsules using ice as sacrificial template were produced by placing with superhydrophobic tweezers the core inside a 4 µL droplet of a MACHI solution above a SA surface. Then, the particle was crosslinked under UV-light (365 nm, 2.8 mW/cm^2) for 1 min using an ice bath below to avoid the core melting prior to the capsule formation. Afterwards, the fabricated particle was placed at RT, which resulted on the ice melting and, hence, on the production of liquid-core MACHI capsule.

S3.2. Liquid-Cores

S3.2.1. *Interfacial Gelation around a $CaCl_2$ droplet*

In a first step, a 2 µL droplet of $CaCl_2$ (1 M in MES buffer) was pipetted to the interior of a 4 µL droplet of diluted ALG solution (0.1% (w/v) in water) in order to produce a flexible layer of ALG around the $CaCl_2$ liquid core by spontaneous ionotropic gelation. In a second step, the coated $CaCl_2$ core was retrieved from the SA surface with hydrophobic tweezers and placed on top of a 4 µL droplet of MACHI (2 w/v% in 16% (v/v) glycerol in

water solution containing 0.25% (w/v) I2959 photoinitiator). The obtained system was subjected to UV-light irradiation (365 nm, 2.8 mW/cm^2) for 1 min to harden the MACHI polymer shell entrapping the liquid core.

S3.3. Hierarchical Polymeric Capsules: Micro/Nanoparticles

S.3.3.1. *Fabrication of the subcompartments*

S3.3.1.1. $CaCO_3$ microparticles

$CaCO_3$ microparticles were synthesized following a well-known method.[28] Shortly, aqueous solutions of sodium carbonate (Na_2CO_3) and calcium chloride ($CaCl_2$) were prepared at 1 M. Coprecipitation of both solutions was performed under vigorous stirring (≈1000 rpm) by mixing 1 mL of each solution. After 30 s, stirring was stopped and the suspension of newly synthesized calcium carbonate ($CaCO_3$) microparticles, as result of growth of polycrystalline spherical vaterite particles,[29] was left to react and precipitate for 15 min. The supernatant was removed and the particles washed twice with ultrapure water to remove residual salts. The obtained capsules were dried at 70ºC until use.

S3.3.1.2. PLLA microparticles

PLLA microparticles were produced by emulsion solvent evaporation technique as elsewhere described with minor modifications.[30] Briefly, 1 g of PLLA was dissolved in 20 mL of CH_2Cl_2 containing a hydrophobic dye, Nile Red. Afterwards, this solution was added under agitation to 100 mL of 0.5% (w/v) PVA and left to stir for 2 days at RT to evaporate the organic solvent. The produced stained PLLA microparticles were collected by filtration and washed several times with distilled water. Ultimately, microparticles were subsequently frozen at −80 °C and lyophilized (Cryodos, Telstar) for 3 days. Prior to usage, microparticles were stored at 4 °C. Prior to usage, microparticles were stored at 4 ºC.

S3.3.1.3. Fe_3O_4 nanoparticles

The production of the Fe_3O_4 nanoparticles was based in a previously described protocol.[31] Shortly, Fe_3O_4 MNPs were synthesized by the co-precipitation reaction of

$FeCl_2 \cdot 4H_2O$ and $FeCl_3 \cdot 6H2O$ salts in the presence of NH_4OH under a nitrogen atmosphere at 60 ºC. The obtained nanoparticles were then washed with deionized water and ethanol for several times, and ultimately dried in a VD23 (Binder, Germany) vacuum oven.

S3.3.2. *Fabrication of Hierarchical MACHI Capsules*

In order to produce hierarchical systems using MACHI capsules as containers of each one of the three types of produced particles, the produced micro/nanoparticles were suspended in a 1.5% (w/v) ALG in water solution. The former solution was dispensed using a pipette (2 µL) above a SA surface and then, the polymeric droplets were cross-linked by adding 2 µL of 0.1 M $CaCl_2$ solution on top of each droplet. Afterwards, the obtained monodisperse templates were assembled inside a MACHI shell followed by the hardening of this polymer coating by UV-exposure for 1 min, yielding capsules after the removal of the template by applying a EDTA treatment. It is worth noticing that glycerol (20% v/v) was added to compensate for the density mismatch.

S3.3.3. *Capsule Mechanical Stability Test*

The mechanical stability of the produced capsules was tested as previously described using a rotational stress test. [32] Two types of capsules thickness were tested, namely 250 µm and 350 µm. The experiments were conducted in triplicates (n=4 for experiment). Therefore, MACHI capsules containing PLLA microparticles (produced as described on Section S3.3.2) were placed inside centrifuge tubes with 5 mL of PBS and, then, centrifuged at 200 rpm for 60 min at RT. Every 15 min, the rotation was stopped in order to assess the number of damage capsules by visual inspection as the shell rupture will be translated on the release of previously entrapped PLLA microparticles inside the ALG sacrificial core. The intact capsules were placed again inside the centrifuge tubes to continue the rotational test.

Figure S5. Results of MACHI capsules stability assay: **A)** Capsules enclosing PLLA microparticles after the rotational assay. As it can be observed the PLLA particles deposited on the MACHI-capsule wall as result of the EDTA treatment. Moreover, non-ruptured capsules were observed since the PLLA particles remained inside the MACHI shell. B) Image of a hydrogel capsule which was ruptured to observe the release of its contents.

S4. Statistical Analysis

The significance of the differences on the average RMS values obtained from Atomic Force Microscopy (AFM) and profilometer was assessed using the Student's t-test. P-values < 0.05 were considered statistically significant. The results are presented as mean ± standard deviation.

References

1. F. Kurayama, S. Suzuki, T. Oyamada, T. Furusawa, M. Sato and N. Suzuki, *J. Colloid Interface Sci*, 2010, **349**, 70-76.
2. C. Li, Z.-Y. Li, J. Zhang, K. Wang, Y.-H. Gong, G.-F. Luo, R.-X. Zhuo and X.-Z. Zhang, *J. Mater. Chem.*, 2012, **22**, 4623-4626.
3. Q. Zhao, B. Han, Z. Wang, C. Gao, C. Peng and J. Shen, *Nanomedicine*, 2007, **3**, 63-74.
4. C. R. Correia, P. Sher, R. L. Reis and J. F. Mano, *Soft Matter*, 2013, **9**, 2125-2130.
5. I. Braccini and S. Pérez, *Biomacromolecules*, 2001, **2**, 1089-1096.
6. K. Y. Lee and D. J. Mooney, *Prog. Polym. Sci.*, 2012, **37**, 106-126.
7. X. Deng, L. Mammen, H.-J. Butt and D. Vollmer, *Science*, 2012, **335**, 67-70.
8. A. M. S. Costa, M. Alatorre-Meda, C. Alvarez-Lorenzo and J. F. Mano, *Small*, 2015, **11**, 3648-3652.
9. A. M. S. Costa, M. Alatorre-Meda, N. M. Oliveira and J. F. Mano, *Langmuir*, 2014, **30**, 4535-4539.
10. A. B. D. Cassie and S. Baxter, *J. Chem. Soc. Faraday Trans.*, 1944, **40**, 546-551.
11. Y. C. Jung and B. Bhushan, *J. Microsc*, 2008, **229**, 127-140.
12. W. Barthlott and C. Neinhuis, *Planta*, 1997, **202**, 1-8.
13. X. Gao and L. Jiang, *Nature*, 2004, **432**, 36-36.

14. M. Nosonovsky and B. Bhushan, *Microelectron. Eng.*, 2007, **84**, 382-386.
15. M. Rinaudo, *Prog. Polym. Sci.*, 2006, **31**, 603-632.
16. L. M. Yu, K. Kazazian and M. S. Shoichet, *J. Biomed. Mater. Res. Part A*, 2007, **82**, 243-255.
17. E. Robles, E. Villar, M. Alatorre-Meda, M. G. Burboa, M. A. Valdez, P. Taboada and V. Mosquera, *J. Appl. Polym. Sci.*, 2013, **129**, 822-834.
18. S. H. Kim and C. C. Chu, *J. Biomed. Mater. Res.*, 2000, **49**, 517-527.
19. A. C. Lima, W. Song, B. Blanco-Fernandez, C. Alvarez-Lorenzo and J. F. Mano, *Pharmaceut Res.*, 2011, **28**, 1294-1305.
20. B. V. Parakhonskiy, A. M. Yashchenok, M. Konrad and A. G. Skirtach, *Adv. Colloid Interface Sci*, 2014, **207**, 253-264.
21. H. Zimmermann, F. Ehrhart, D. Zimmermann, K. Müller, A. Katsen-Globa, M. Behringer, P. J. Feilen, P. Gessner, G. Zimmermann, S. G. Shirley, M. M. Weber, J. Metze and U. Zimmermann, *Appl. Phys. A*, 2007, **89**, 909-922.
22. F. Caruso, *Chem. Eur. J*, 2000, **6**, 413-419.
23. J. Cui, M. P. van Koeverden, M. Müllner, K. Kempe and F. Caruso, *Adv. Colloid Interface Sci.*, 2014, **207**, 14-31.
24. E. C. Goethals, A. Elbaz, A. L. Lopata, S. K. Bhargava and V. Bansal, *Langmuir*, 2013, **29**, 658-666.
25. F. Bode, M. A. da Silva, A. F. Drake, S. B. Ross-Murphy and C. A. Dreiss, *Biomacromolecules*, 2011, **12**, 3741-3752.
26. A. Duconseille, T. Astruc, N. Quintana, F. Meersman and V. Sante-Lhoutellier, *Food Hydrocolloid.*, 2015, **43**, 360-376.
27. X. Liu and P. X. Ma, *Biomaterials*, 2009, **30**, 4094-4103.
28. R. R. Costa, E. Castro, F. J. Arias, J. C. Rodríguez-Cabello and J. F. Mano, *Biomacromolecules*, 2013, **14**, 2403-2410.
29. J.-P. Andreassen, *J. Cryst. Growth*, 2005, **274**, 256-264.
30. R. Bodmeier and J. W. McGinity, *J. Microencapsul.*, 1988, **5**, 325-330.
31. S. Gil, E. Castro and J. F. Mano, *Mater. Lett.*, 2013, **100**, 266-270.
32. T. Haque, H. Chen, W. Ouyang, C. Martoni, B. Lawuyi, A. M. Urbanska and S. Prakash, *Mol. Pharm.*, 2005, **2**, 29-36.